Binary Grating of Subwavelength Silver and Quantum Wires as a Photonic-Plasmonic Lasing Platform With Nanoscale Elements

Volodymyr O. Byelobrov, *Student Member, IEEE*, Trevor M. Benson, *Senior Member, IEEE*, and Alexander I. Nosich, *Fellow, IEEE*

Abstract—This paper considers the scattering of an H-polarized plane wave by a freestanding periodic grating that contains two circular cylinders on each period, one made of silver and the other of dielectric. If such a grating is made of deeply subwavelength wires, the reflection and transmission coefficients demonstrate both plasmon and grating resonances. To clarify them, we also discuss the scattering by similar gratings made of either silver or dielectric wires only. However, the main attention is paid to the associated lasing eigenvalue problem for the dielectric cylinders pumped to become quantum wires, i.e., to obtain a "negative-absorption" complex refractive index. The analysis is done using a meshless analytical-numerical method with guaranteed convergence. The computations show that, in this composite periodic cavity, material thresholds of lasing for the grating modes can be much lower than for the plasmon modes.

Index Terms—Gratings, lasing, nanowires, plasmons, scattering, threshold.

I. INTRODUCTION

TRULY nanoscale lasers were recently demonstrated in the form of a random ensemble of spherical gold particles, each of 14-nm diameter and coated with a spherical layer of dye-doped silica [1]. Other configurations of lasers actively discussed today are rather *subwavelength* than truly nanosize, as they use the lowest modes of semiconductor disks or short rods encapsulated into metal cases [2]–[4]. The nanowire and photonic-crystal nanodefect-cavity lasers are even further from the nanoscale because one or two of their physical dimensions are of the order of several microns; hence, they are rather *microlasers with nanoscale features*. In fact, the only physical mechanism able to provide a confinement of light on the nanoscale is the localized surface-plasmon resonance. Still as the output power generally scales with the device size, and because the
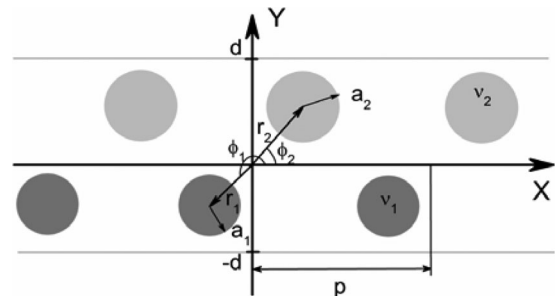
Fig. 1. Geometry of infinite binary grating of circular cylinders (wires) made of materials with different refractive indices.

noble-metal cores or shells have considerable losses, one of discussed ways today to build a practical device is to assemble elementary nanolasers in groups or arrays. Such an arrangement obviously leads to the microscale dimensions along at least one coordinate. However, it brings new physics in the form of different resonances caused by the periodicity. Therefore, the aim of this paper is the quantification and comparison of the thresholds of the natural modes of a laser configuration with deeply nanoscale elements: a binary grating made of circular wires of two types (see Fig. 1), one silver and the other a dielectric-with-gain or a quantum wire (QW).

Although such a laser also has two physical dimensions larger than nanoscale, it can be viewed as a 2-D analog of a binary chain of silver particles and quantum dots. A study of infinite grating is also important as a theoretical limiting case for finite gratings of many nanoscale elements.

Existing technologies enable the manufacture of active regions in semiconductor microcavities shaped as cascaded quantum wells and, since recently, as periodic arrays of QWs. If pumped, such wires can display an inversed population of carriers that can be expressed as negative absorption or bulk material gain. It is known that lasing occurs on discrete frequencies, associated with the natural modes (a.k.a. the eigenmodes) of the optical cavity, if the pump power is above the threshold. Therefore, lasing can be studied as an eigenvalue problem, modified for the presence of the active region. This problem is referred to as a lasing eigenvalue problem (LEP) and has been discussed in [5], [6]. We will apply this formalism to the study of configuration of Fig. 1.

Here, the analysis of the auxiliary problem of the scattering of light is important. This is because it reveals the natural-mode resonances in the scattering characteristics, and thus provides

initial-guess approximations for the numerical search of LEP eigenvalues in the presence of QWs. In turn, the analysis of the scattering by gratings made of only dielectric or silver wires is instrumental in the understanding of binary grating.

Although numerous publications have studied the classical transmission and reflection of plane waves by infinite gratings of passive dielectric and metallic wires of circular cross section (for instance, see [7]–[9]), the first direct mention of the so-called grating resonances close to (however never coinciding with) the Rayleigh anomalies occurred in [10]–[12]. More recently, we have studied the associated LEP for the lasing modes of an infinite grating made of circular QWs [13]. We found a nonobvious effect: the lowering of the lasing thresholds of the grating modes in the periodic structure if the wire radius decreases or, equivalently, the relative volume of the active media gets smaller. Additionally, a grating of quantum wires has lower lasing thresholds for the grating modes in the H-polarization case; this is explained by the nonmagnetic nature of QWs.

For a grating of silver wires, the plane-wave scattering analysis shows coexistence, in the visible range, of the low-quality single-wire plasmon resonances and the high-quality collective ones, i.e., the grating resonances [14]. In particular, by tuning two resonances nearer to each other one can observe a great variety of Fano shapes in the reflectance spectra.

Here, we investigate a novel type of periodic resonator by placing silver and dielectric wires of nanoscale diameter in one period. For the silver nanowires, the values of the bulk material refractive index in the visible band are taken from [15] and interpolated using cubic splines. The LEP is formulated by adding a negative imaginary part (lasing threshold γ) to the bulk refractive index of dielectric wires and seeking it jointly with the lasing frequency σ. We call these values the LEP eigenpairs; they are discrete and each of them corresponds to a specific mode. If the wires diameter is deeply subwavelength, then the modes connected with the electromagnetic field locked inside one cylinder in free space are absent (have very high thresholds), and only the modes caused by the periodicity of the grating and the plasmonic nature of silver are relevant. To find the initial-guess values for the LEP eigenpairs, we use the frequencies of high reflection in the auxiliary scattering problem where the refractive index of the dielectric wires remains real valued.

The remaining part of this paper is structured as follows. In Section II, we present the formulation, the basic equations, and a short review of the obtained numerical results for the plane-wave scattering problems associated with passive wire gratings. Section III addresses the LEP for a binary grating of silver wires and QWs. Conclusions are collected in Section IV.

II. SCATTERING BY PERIODIC GRATINGS

A. Scattering Problem Formulation

Consider a grating made of circular cylinders (wires) in free space lying in parallel to the z-axis and periodically along the x-axis with period p (see Fig. 1). If there is a single cylinder per period, then we denote its radius as a and its refractive index as ν. Otherwise these parameters obtain indices 1 and 2. The field is assumed time harmonic as $\sim \exp(-i\omega t)$ and does

not vary along the z-axis, so the field analysis is 2-D. Keeping in mind plasmon resonances, we investigate the scattering of the H-polarized plane wave incident from the upper half-space along the y-axis. The function U, denoting the H_z component of the electromagnetic field, must satisfy the Helmholtz equation with appropriate wavenumber inside and outside of cylinders, the Sveshnikov radiation condition at infinity [16], [17], the condition of local integrability of power, and the boundary conditions demanding continuity of the tangential field components at the wire boundaries. As we consider normal incidence, then the Floquet theorem tells that the scattered field is a periodic function of x with period p: $U(x,y) = U(x+p,y)$. In this case, we can investigate the field just within one cell of the grating. The free space wavenumber is $k = \omega/c = 2\pi/\lambda$, where c is the free-space light velocity and λ is the wavelength, while inside the cylinders it is $k\nu_{1,2}$. In this paper, we will also use the normalized frequency, $\sigma = p/\lambda = kp/2\pi$.

B. Basic Equations

Consider at first a grating with identical wires. The field in the vicinity of the cylinder is naturally expanded into angular-exponent series with the cylindrical functions in coefficients (inside the wires the Bessel functions and outside the Hankel functions of the first kind) [7]–[9], [13], [14]. However, such series are not a convenient tool for large values of the variable $|y|$.

Therefore, the Poisson summation formula is applied to cast the series into the exponentially convergent series in terms of the Floquet harmonics [7]–[9]. Then, the field function in the upper and lower half-spaces (out of the grating domain) is presented in the following way:

$$U^{\pm}(x,y) = \sum_{s=-\infty}^{+\infty} f_s^{\pm} e^{ik(\pi_s x + \tau_s |y|)}, \quad \pm y > d \quad (1)$$

$$\pi_s = \frac{s}{\sigma}, \quad \tau_s = (1 - \pi_s^2)^{1/2} \quad (2)$$

and width d corresponds to the strip containing all wires.

Considering the field near a single cylinder, we can see that it consists of two components: first the incident field and second the field scattered from the rest of the infinite chain of wires, i.e., from all cylinders except the one considered. Combining and matching these fields, we find that the vector of the expansion coefficients X of the field scattered by a single wire of the infinite chain satisfies the matrix equation

$$(I - J^{-1} \cdot S \cdot L \cdot J) \cdot X = S \cdot J^{-1} \cdot P \quad (3)$$

with

$$L = [L_{m-n}(2\pi\sigma)] \quad (4)$$

$$S(\nu, a) = \left[-\frac{\nu^{-1} J_m(ka) J_m'(k\nu a) - J_m'(ka) J_m(k\nu a)}{\nu^{-1} H_m(ka) J_m'(k\nu a) - H_m'(ka) J_m(k\nu a)} \delta_n^m \right] \quad (5)$$

$$P = [(-1)^m] \quad (6)$$

$$J = [J_m(2\pi\sigma)\delta_n^m] \quad (7)$$

where δ_n^m is the Kronecker symbol, and the matrix L consists of the lattice sums, which provide a rapid way of summing the slowly converging Hankel function series (for details see [18], [14]). This matrix reflects the periodic nature of the grating and depends only on the value $\sigma = p/\lambda$. The matrix S corresponds to the scattering of the plane wave by a single cylinder in free space with radius a and refractive index v. The vector P corresponds to the incident plane wave. Besides, we establish the expressions that transform the expansions of the scattered field in terms of the Fourier–Hankel series to those in terms of the Floquet series

$$f^{\pm} = F^{\pm} \cdot J \cdot X \qquad (8)$$

$$F^{\pm} = (\pi\sigma)^{-1}[(-i\pi_n \pm \tau_n)^m]. \qquad (9)$$

Note that the matrix (3) is identical to those used in [13], [14], but written in operator notation. It differs from the equations used in [7]–[9] by the involvement of the diagonal matrix J. This guarantees the satisfaction of the Fredholm conditions and hence the convergence of numerical solution.

The values of reflectance and transmittance can be obtained using (1) as follows:

$$R = \sum_{s<\sigma} \tau_s |f_s^+|^2, \quad T = \sum_{s<\sigma} \tau_s |\delta_s^0 - f_s^-|^2 \qquad (10)$$

and absorbance can be obtained from the optical theorem (power conservation law) as $A = 1 - R - T$.

C. Plane-Wave Scattering Characteristics

At first, we investigate a dielectric-wire grating in free space. The relief in Fig. 2(a) shows the variation of the reflectance of such a grating with period $p = 400$ nm and wire refractive index $\nu = 2.48$ as a function of the wavelength and the wire radius. Here, the bright ridges mark the resonances of enhanced reflection. If the wire radius gets smaller, the most intense of them tend to the multiples of the value $\sigma = 1$ or $\lambda = p$. These are the grating resonances [10]–[14]. Though Fig. 2(a) shows two distinct grating resonances near $\lambda = p$, we investigate the first one as it shows a longer "life" before disappearing in the branch point $\sigma = 1$. It corresponds to the eigenmode whose H-field is symmetric across the x-axis [13]. The main feature of this grating resonance is that the total field rises not just in the vicinity of the wires but also between them. In the grating resonance near to $\sigma = 1$, the Floquet harmonics of the first orders dominate greatly, $|f_{\pm1}^{\pm}| = O(Q_G) \gg |f_{s\neq\pm1}^{\pm}|$ ($Q_G \gg 1$ being the quality factor [14]), and therefore the near field is

$$U(x,y) \approx f_{\pm1}^{\pm} \cos(k\pi_1 x) \approx Q_G \cos\left(\frac{2\pi x}{p}\right). \qquad (11)$$

Such a pattern is seen on the near-field portraits in Fig. 2(b) and (c). In (b), a spot of high intensity between cylinders appears, and in (c) the standing wave (11) is clearly visible.

The silver-wire grating is investigated using the same equations as for the dielectric one except that the refractive index for the wires is taken from the experimental data of [15].

The relief of reflectance in Fig. 3(a) shows the interaction of two kinds of resonances: the plasmon resonance observed
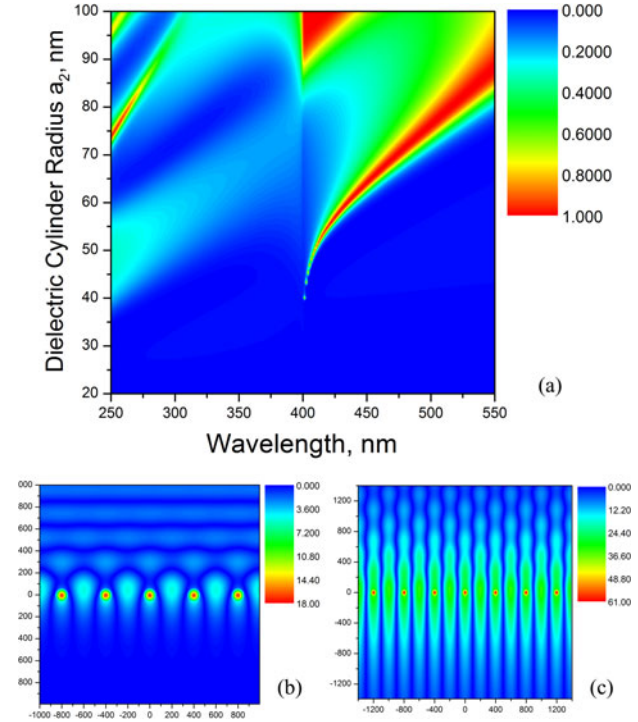

Fig. 2. Relief of reflectance of the normally incident plane wave for the dielectric-wire grating with $\nu = 2.48$ and period $p = 400$ nm (a) as a function of the wire radius and the wavelength. The near field patterns for the grating resonance corresponding to (b) $a = 60$ nm, $\lambda = 434.8$ nm and (c) $a = 40$ nm, $\lambda = 401.3$ nm.

near the wavelength of $\lambda \approx 340$ nm, and the grating one near $\lambda = p = 400$ nm. Together they form a wide spectral band of high reflectance followed by an abrupt drop (a sort of double-extremum Fano-shape dependence). More results on this effect, with a deeper discussion, can be found in [14].

The associated relief of absorbance in Fig. 3(b) gives additional information. The absorbance is high if the ratio of the silver-wire radius to period is large and the wavelength is in the violet, where bulk losses in silver are larger. The two resonances mentioned earlier are also clearly visible. Note that in-resonance absorbance is quite comparable to reflectance.

The near field patterns are shown for the wires of radius $a = 50$ nm in the plasmon resonance at $\lambda = 340$ nm and in the grating one at $\lambda = 399$ nm. In the first resonance, we see the concentration of the field on the upper side of the wires that faces the incident wave. In addition to the main (zero) diffractive order, here the $\pm$1st Floquet harmonics are also propagating as $\lambda < p$. The pattern in the second resonance is reminiscent of Fig. 2(c) in the sense of forming a cosine-like field pattern, but because of the presence of absorption it is more intense in the upper half-plane.

These interesting resonance effects of the two different gratings obviously merge together in the scattering by a binary grating shown in Fig. 1. As the geometry of the elementary cell is involved in (3) through the operator S, one should only modify this operator to analyze such a modified grating. We can derive the required scattering matrix for several cylinders
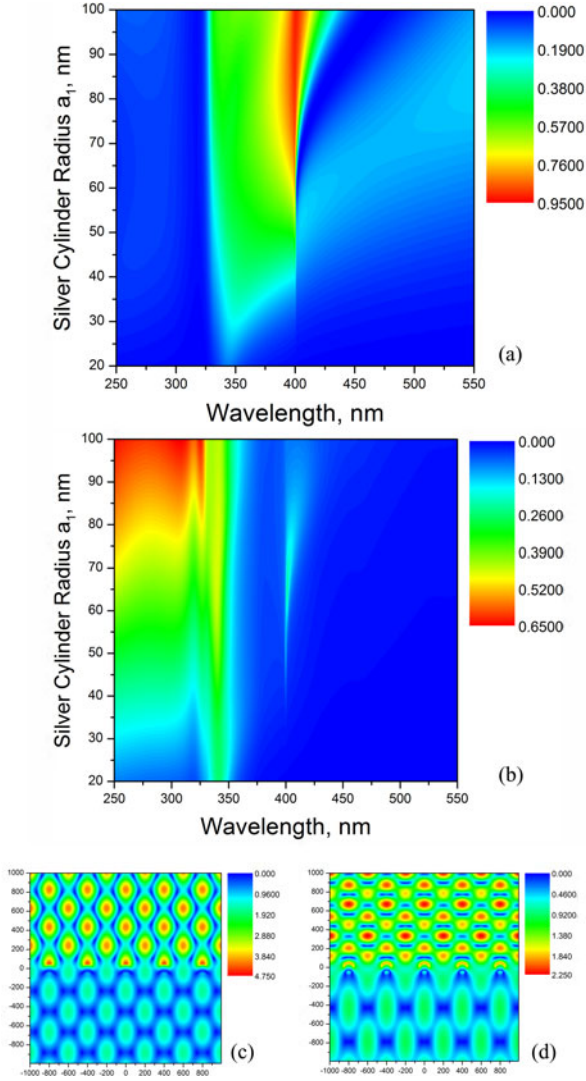
Fig. 3. (a) Reliefs of reflectance, and (b) absorbance of a plane wave normally incident on the silver-wire grating and the near field patterns for $a = 50$ nm at the wavelengths of (c) $\lambda = 340$ nm and (d) $\lambda = 399$ nm.
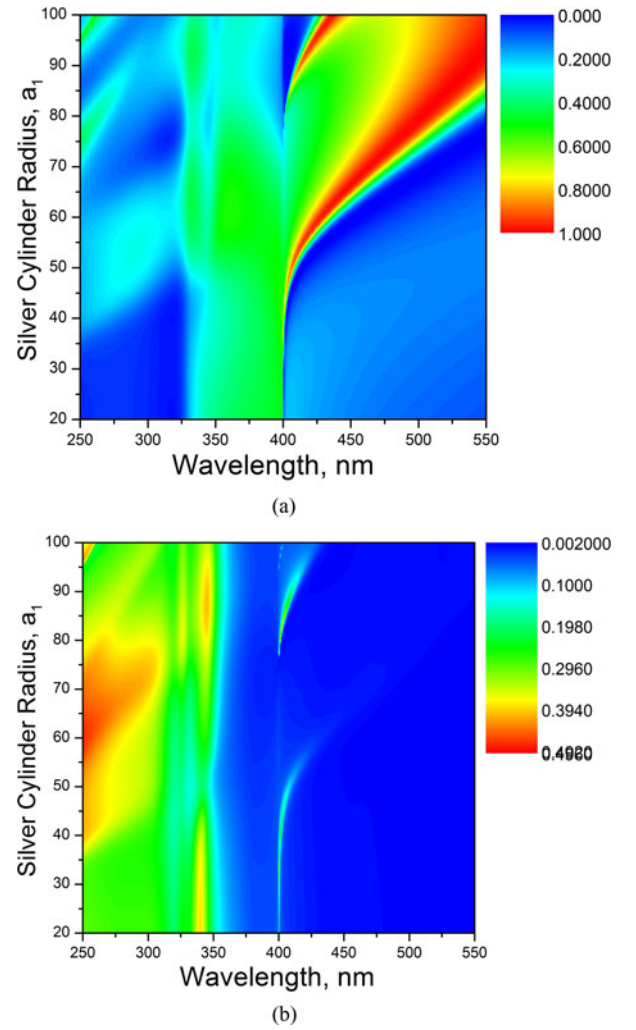

Fig. 4. (a) Reliefs of reflectance and (b) absorbance of the binary grating of silver and dielectric wires with $p = 400$ nm. Silver wire is placed at $r_1 = 100$ nm, $\phi_1 = 0$, and $a_1 = 50$ nm. Dielectric wire with index $\nu = 2.48$ is at $r_2 = 100$ nm, $\phi_1 = \pi$, and has varying period a_2.

in free space following the approach presented in [19]. Assume that there are two wires per period having radii a_1 and a_2, their centers are located at $\vec{r}_{1,2} = (r_{1,2}, \phi_{1,2})$ with respect to the cell origin, and their refractive indices are v_1 and v_2, respectively. Then, S should be replaced in (5) with

$$\bar{S} = \beta_{0,1}\tilde{S}^1 + \beta_{0,2}\tilde{S}^2 \tag{12}$$

$$\tilde{S}^1 = (I - S^1\alpha_{1,2}S^2\alpha_{2,1})^{-1}S^1(\beta_{1,0} + \alpha_{1,2}S^2\alpha_{2,1}) \tag{13}$$

$$\tilde{S}^2 = (I - S^2\alpha_{2,1}S^1\alpha_{1,2})^{-1}S^2(\beta_{2,0} + \alpha_{2,1}S^1\alpha_{1,2}) \tag{14}$$

where $S^i = S(\nu_i, a_i)$ is still given by (5), and if the wire material is silver, then $\nu = \nu(\lambda)$. Furthermore

$$\alpha_{i,j} = [H_{n-m}(k|\vec{r}_i - \vec{r}_j|)e^{i(n-m)\mathrm{Arg}(\vec{r}_i - \vec{r}_j)}] \tag{15}$$

$$\beta_{0,i} = [J_{n-m}(k|\vec{r}_i|)e^{-i(n-m)\mathrm{Arg}(\vec{r}_i)}] \tag{16}$$

$$\beta_{i,0} = [J_{n-m}(k|\vec{r}_i|)e^{i(n-m)\mathrm{Arg}(\vec{r}_i)}]. \tag{17}$$

First, we investigate the structure where the two wires are placed in the plane of the grating with $p = 400$ nm. The silver wire has a fixed radius, $a_1 = 50$ nm, and is placed 100 nm to the right of the cell center, i.e., $r_1 = 100$ nm, $\phi_1 = 0$. The dielectric cylinder with varying radius a_2 has its center at $r_2 = 100$ nm, $\phi_2 = \pi$. The reliefs of the dependences of reflectance and absorbance on a_2 and wavelength λ are shown in Fig. 4(a) and (b), respectively. Here, one can see that the reflectance behavior inherits all the resonances mentioned before for the two different gratings of identical wires. Still their interaction is far from obvious.

We have also investigated the case of wires being rotated around the cell origin. The reliefs of reflectance and absorbance as a function of the wavelength and their position angle are shown in Fig. 5(a) and (b). Here, both wires have the same radii, $a_1 = a_2 = 50$ nm, and both are placed 100 nm away from the cell center in symmetric manner. Their position is characterized by the rotation angle ϕ as $\phi_1 = \phi$ and $\phi_2 = \pi + \phi$. One can see that the band of high reflectance between the plasmon and
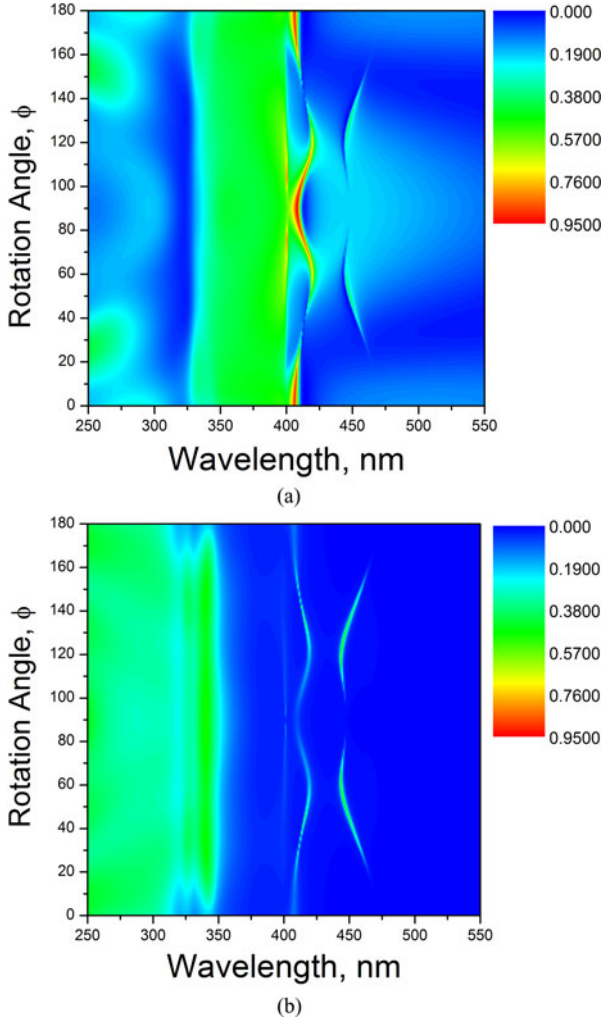
Fig. 5. (a) Reliefs of reflectance and (b) absorbance (b) of the binary grating of silver and dielectric wires with $p = 400\,\text{nm}$. Silver wire is placed at $r_1 = 100\,\text{nm}$, $\phi_1 = \phi$, and $a_1 = 50$. Dielectric wire with refractive index $\nu = 2.48$ has its center at $r_1 = 100\,\text{nm}$, $\phi_1 = \phi + \pi$. The wire radii are $a_1 = a_2 = 50$.

the grating resonances stays fixed for any value of the rotation angle ϕ.

The grating resonances define themselves as two varying in position ridges to the right of $\lambda = p$. Note that the resonance on the larger wavelength disappears at $\phi = 0$, $\pi/2$ and, π, i.e., if the silver and dielectric wires are in stacked and in-plane arrangements. This can be explained if the associated mode tends to the x-antisymmetric mode at $\phi \to 0$, $\pi/2$, and π, and thus is not excited by the normally incident plane wave.

III. LASING EIGENVALUE PROBLEM

The classical scattering eigenproblem implies calculation of the complex-valued natural-mode frequency as an eigenvalue [5], [6]. Then, the imaginary part of the frequency corresponds to the radiation losses and losses in imperfect scatterers, say, mirrors. At the lasing threshold, the eigenfrequency should take a purely real value; this can be achieved if one applies some pumping necessary to create material gain and compensate for
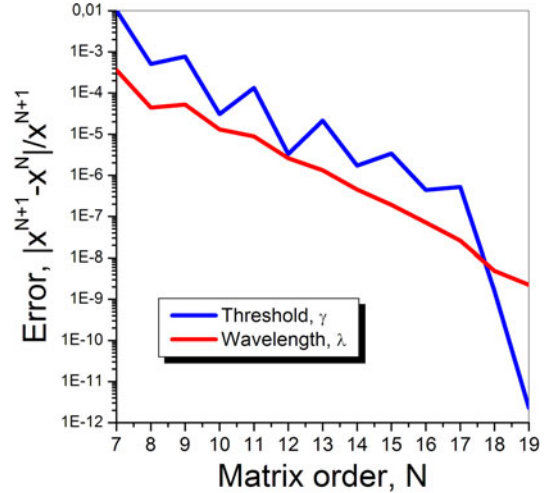

Fig. 6. Computational errors versus the matrix truncation order N for the components of LEP eigenvalue corresponding to the first grating mode of a binary grating with the same parameters as in Fig. 4..

both radiation and absorption. In [5] and [6], a more straight-forward way was proposed to study the eigenmodes of open resonators used in lasers. Suppose the resonator has a region filled with an active material meaning its bulk refractive index has strictly negative imaginary part, $\nu = \alpha - i\gamma$. Then, one can consider the modal frequency and the bulk material gain γ at the threshold as an eigenvalue pair in the equations of the classical problem, analytically continued to all complex-valued refractive indices. Hence, the lasing frequency, as well as the threshold, is obtained in one step. For more details refer to [5], [6], and [13].

For an infinite grating containing QWs, the LEP eigenvalue pairs (λ, γ) satisfy the following determinantal equation:

$$\det(I - J^{-1} \cdot \bar{S} \cdot L \cdot J) = 0. \qquad (18)$$

This binary-grating equation is a generalization of that used in [13] for the analysis of a grating of QWs in free space. Note that, thanks to the Fredholm second-kind nature of the matrix generating (18), the infinite-dimension determinant exists as a function of parameters, and roots of (18) can be approached by solving the truncated equations of progressively larger size.

This is illustrated by the plots in Fig. 6 where the relative computational error is shown as a function of the matrix truncation order N for the grating-mode frequency and threshold in the case of all wires located in the same plane, $a_1 = a_2 = 50\,\text{nm}$ and $\nu = 2.48$.

Fig. 7 shows the plots of eigenpairs for the same variation of geometry as in Fig. 4, i.e., for all wires placed in the same plane. The curves in Fig. 7(a) show that the lasing wavelength of the lowest x-symmetric grating mode in the purely QW and in the binary gratings have almost the same values—they are hardly distinguishable from each other. This is unlike the thresholds of the same modes shown in Fig. 7(b), for the QW grating, they monotonically decay if shrinking the wire radius (see [13]); however, for the binary grating they reach a minimum value and then start growing. The explanation can be found in the
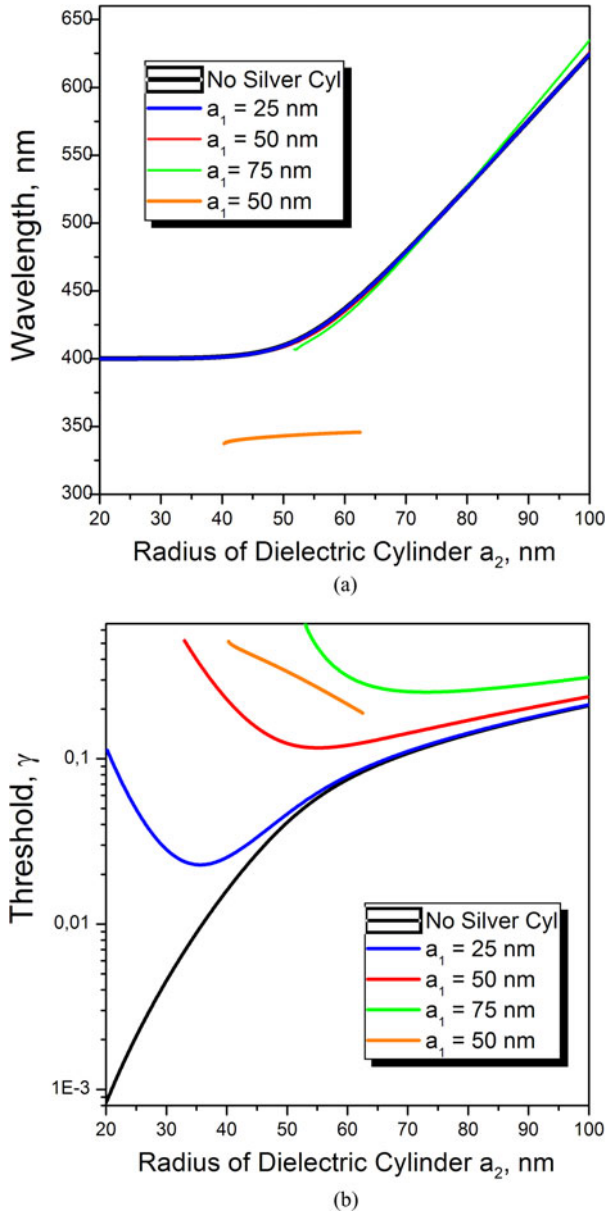
Fig. 7. LEP eigenpairs versus the QW radius: black line corresponds to the grating mode for the QW grating. The colored lines are for two wires per period, one QW and another of silver, where the first has the radius a_2 varying from 100 to 20 nm and the centre away 100 nm from the origin and the silver wire has a constant radius (see inset) and its centre is just symmetrically opposite from origin, the period is 400 nm. The shorter curve is for the plasmon mode.

Fig. 8. Same geometry as in Fig. 5: (a) lasing wavelengths and (b) thresholds as a function of the rotation angle for the binary grating.

fact that in the binary-grating case the pumping of the active dielectric cylinders has to overcome the losses in the silver wires in addition to the radiative losses. Interestingly enough, the minimum of the threshold is reached if the wires have roughly equal radii.

To consider a binary grating as a photonic-plasmonic lasing platform with nanoscale elements, it is necessary to quantify the lasing thresholds of all possible eigenmodes of this structure. The shorter curves in Fig. 7 correspond to the plasmon mode (as clear from its wavelength) whose threshold happens to be higher than for the grating mode.
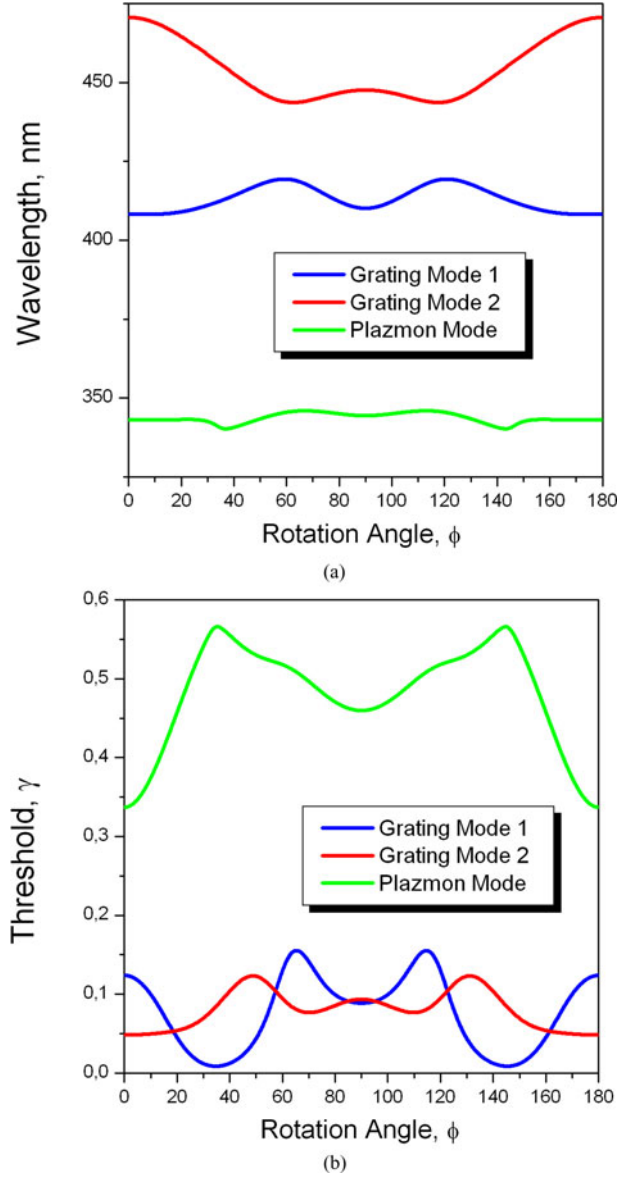
To compare the plasmon mode with the grating modes in more detail, we have studied the effect of rotation of the pair of wires around the cell center. Fig. 8 shows interesting dependences of three different LEP eigenpairs on the angle of rotation, where the binary-grating geometry is the same as in the plane-wave scattering problem corresponding to Fig. 5.

Here, the lasing wavelengths enable us to easily identify the modes: the plasmon mode keeps its wavelength near to $\lambda \approx 340$ nm, while two other modes are the grating modes because their wavelengths are above the $\lambda = p = 400$ nm value. Note that mode 1 is the same as the one studied in Fig. 7 and mode 2 is another one whose presence can be seen as a broad low ridge in the right-lower corner of Fig. 4(a).

The lasing threshold curves follow the same tracks as the high-reflection resonances in Fig. 5(a), as could be expected. Mode 1 has a local minimum in the stacked arrangement case of

$\phi = \pi/2$. However, a deeper minimum lies at a different angle of the inclined arrangement. It may be understood through the analysis of the areas of high-intensity field near to the wires. Note that according to (11), the x-symmetric grating-mode H-field has a strong maximum between the wires for mode 1. As is known, the electric field has zeros where the magnetic field has maximum values. Therefore, placing the QWs in the middle between the silver wires should provide a poor overlap between the mode electric field and the active region for mode 1. Mode 2 has the opposite symmetry across the y-axis at $\phi = \pi/2$, and therefore its threshold behavior in Fig. 8(b) is different. Note also that modes 1 and 2 display a parametric interaction under the variation of angle ϕ: their wavelengths come nearer at the same values of angle where their thresholds cross each other.

The most important observation is that the threshold for the plasmon mode is generally some 3 to 60 times higher than for the grating modes, at least if all wire radii are 50 nm.

Thus, the behavior of the thresholds of all three modes of a binary grating considered here is in good agreement with the position of QW in the corresponding near-field mode pattern (such patterns resemble those in Fig. 3(b) and (c) because a thin QW is a small perturbation). For the link between the overlap coefficient and the mode threshold, see [6] where thresholds are explained with the aid of the optical theorem applied to the LEP solutions.

IV. CONCLUSION

We have presented results of numerical study, by a mesh-less method with guaranteed convergence, of the behavior of the lasing wavelengths and thresholds of the grating-type and the plasmon-type modes in a binary grating formed of pairs of silver and quantum wires. The main result obtained is that the thresholds of the grating or "collective" modes can be comparable to and lower than the threshold of the main plasmon-type lasing mode associated with the noninteracting silver wires. As we believe, this may clarify what can be expected from periodic microlasers with nanoscale elements. Unlike a purely quantum-wire grating, here the grating-mode threshold increases if the radius of the QW gets smaller than a certain value depending on the radius of the silver wire. Still in finite gratings the grating mode thresholds can be affected by not sufficiently large number of periods used. This question needs a further study.

REFERENCES

[1] M. A. Noginov, G. Zhu, A. M. Belgrave, R. Bakker, V. M. Shalaev, E. E. Narimanov, S. Stout, E. Herz, T. Suteewong, and U. Wiesner, "Demonstration of a spaser-based nanolaser," *Nature*, vol. 460, pp. 1110–1112, 2009.

[2] M. P. Nezhad, A. Simic, O. Bondarenko, B. Slutsky, A. Mizrahi, L. Feng, V. Lomakin, and Y. Fainman, "Room-temperature subwavelength metal-lodielectric lasers," *Nature Photon*, vol. 4, pp. 395–399, 2010.

[3] M. T. Hill, "Status and prospects for metallic and plasmonic nano-lasers," *J. Opt. Soc. Amer. B*, vol. 27, no. 10, pp. 36–44, 2010.

[4] S. W. Chang, T. R. Lin, and S. L. Chuang, "Theory of plasmonic Fabry–Perot nanolasers," *Opt. Exp.*, vol. 18, no. 14, pp. 15039–15053, 2010.

[5] A. I. Nosich, E. I. Smotrova, S. V. Boriskina, T. M. Benson, and P. Sewell, "Trends in microdisk laser research and linear optical modeling," *Opt. Quantum Electron.*, vol. 39, no. 15, pp. 1253–1272, 2007.

[6] E. I. Smotrova, V. O. Byelobrov, T. M. Benson, P. Sewell, J. Ctyroky, and A. I. Nosich, "Optical theorem helps understand thresholds of lasing in microcavities with active regions," *IEEE J. Quantum Electron.*, vol. 47, no. 1, pp. 20–30, Jan. 2011.

[7] V. Twersky, "On scattering of waves by the infinite grating of circular cylinders," *IRE Trans. Antennas Propagat.*, vol. 10, no. 6, pp. 737–765, 1962.

[8] O. Kavaklioglu, "On diffraction of waves by the infinite grating of circular dielectric cylinders at oblique incidence: Floquet representation," *J. Modern Phys.*, vol. 48, pp. 125–142, 2001.

[9] H. Toyama and K. Yasumoto, "Electromagnetic scattering from periodic arrays of composite circular cylinders with internal cylindrical scatterers," *Prog. Electromagn. Res.*, vol. 52, no. 10, pp. 321–333, 2005.

[10] R. Gomez-Medina, M. Laroche, and J. J. Saenz, "Extraordinary optical reflection from sub-wavelength cylinder arrays," *Opt. Exp.*, vol. 14, pp. 3730–3737, 2006.

[11] M. Laroche, S. Albaladejo, R. Gomez-Medina, and J. J. Saenz, "Tuning the optical response of nanocylinder arrays: An analytical study," *Phys. Rev. B*, vol. 74, p. 245422(5), 2006.

[12] M. Laroche, S. Albaladejo, R. Carminati, and J. J. Saenz, "Optical resonances in one-dimensional dielectric nano-rod arrays: Field-induces fluorescence enhancement," *Opt. Lett.*, vol. 32, pp. 2762–2764, 2007.

[13] V. O. Byelobrov, J. Ctyroky, T. M. Benson, A. Altintas, R. Sauleau, and A. I. Nosich, "Low-threshold lasing modes of an infinite periodic chain of quantum wires," *Opt. Lett*, vol. 35, no. 21, pp. 3634–3636, 2010.

[14] D. M. Natarov, V. O. Byelobrov, R. Sauleau, T. M. Benson, and A. I. Nosich, "Periodicity-induced effects in the scattering and absorption of light by infinite and finite gratings of circular silver nanowires," *Opt. Exp.*, vol. 19, no. 22, pp. 22176–22190, 2011.

[15] P. B. Johnson and R. W. Christy, "Optical constants of the noble metals," *Phys. Rev.*, vol. 6, pp. 4370–4379, 1972.

[16] A. G. Sveshnikov, "Limiting absorption principle for a waveguide," *Doklady Akademii Nauk SSSR*, vol. 80, no. 3, pp. 341–344, 1951.

[17] A. I. Nosich, "Radiation conditions, limiting absorption principle, and general relations in open waveguide scattering," *J. Electromagn. Waves Appl.*, vol. 8, no. 4, pp. 329–353, 1994.

[18] C. M. Linton, "The Green's function for the 2-D Helmholtz equation in periodic domains," *J. Eng. Math.*, vol. 33, pp. 377–402, 1998.

[19] W. C. Chew, *Waves and Fields in Inhomogeneous Media*. New York: Van Nostrand Reinhold, 1990.

Volodymyr O. Byelobrov (S'07) was born in 1983 in Kharkiv, Ukraine. He received the M.Sc. degree in mathematics from the Kharkiv National University, Kharkiv, in 2005. He is currently working toward the Ph.D. degree (part time) at the Laboratory of Micro- and Nanooptics, Institute of Radio-Physics and Electronics, National Academy of Sciences of Ukraine, Kharkiv.

He is also a Research Engineer in the Laboratory of Micro- and Nanooptics. His current research interests include electromagnetic properties of periodic structures, Bragg reflectors, plasmon resonances, eigenvalue problems, and lasing.

Dr. Byelobrov received the IEEE Antennas and Propagation Society Doctoral Research Award in 2007, the International Visegrad Fund Scholarship in 2009, and the European Science Foundation Exchange Grant in 2011.

Trevor M. Benson (M'95–SM'01) received the Ph.D. degree in electronic and electrical engineering from the University of Sheffield, Sheffield, U.K., in 1982 and the D.Sc. degree from the University of Nottingham, Nottingham, U.K., in 2005.

After spending more than six years as a Lecturer at University College Cardiff, he moved to the University of Nottingham in 1989. Since October 2011, he has been the Director of the George Green Institute for Electromagnetics Research, University of Nottingham. His research interests include experimental and numerical studies of electromagnetic fields and waves with emphasis on the theory, modeling and simulation of optical waveguides, nanoscale photonic circuits, and electromagnetic compatibility.

Dr. Benson is a Fellow of the Institute of Electrical Engineering (FIEE) and the Institute of Physics (FInst.P). He was elected a Fellow of the Royal Academy of Engineering in 2005 for his achievements in the development of versatile design software used to analyze propagation in optoelectronic waveguides and photonic integrated circuits.

Alexander I. Nosich (M'94–SM'95–F'04) was born in 1953 in Kharkiv, Ukraine. He received the M.S., Ph.D., and D.Sc. degrees in radio physics all from the Kharkiv National University, Kharkiv, in 1975, 1979, and 1990, respectively.

Since 1979, he has been at the Institute of Radio Physics and Electronics of the National Academy of Science of Ukraine, Kharkiv, where he is currently a Professor and the Principal Scientist heading the Laboratory of Micro- and NanoOptics. Since 1992, he has held a number of Guest Fellowships and Professorships in the EU, Japan, Singapore, and Turkey. His research interests include the method of analytical regularization, propagation and scattering of waves, open waveguides, and lasers and antennas.

Dr. Nosich is a Senior Member of the Optical Society of America. He was one of the Initiators and the Technical Committee Chairman of the International Conference Series on Mathematical Methods in Electromagnetic Theory (MMET). In 1995, he organized the IEEE AP-S East Ukraine Chapter, the first one in the former USSR. He currently represents Ukraine in the European Association on Antennas and Propagation.